DOI: 10.1002/anie.201400655

Magnetic Anisotropy

Large Zero-Field Splittings of the Ground Spin State Arising from Antisymmetric Exchange Effects in Heterometallic Triangles**

*Samantha A. Magee, Stephen Sproules, Anne-Laure Barra, Grigore A. Timco, Nicholas F. Chilton, David Collison, Richard E. P. Winpenny, and Eric J. L. McInnes**

Abstract: *$[Ru_2Mn(O)(O_2CtBu)_6(py)_3]$ has an $S={}^5\!/_2$ ground state with a very large zero-field splitting (ZFS) of $D=2.9\,cm^{-1}$, as characterized by EPR spectroscopy at 4–330 GHz. This is far too large to be due to the Mn^{II} ion ($D<0.2\,cm^{-1}$), as shown from the $\{Fe_2Mn\}$ analogue, but can be modeled by antisymmetric exchange effects.*

The magnetic anisotropy in transition-ion clusters is of fundamental importance in areas such as molecular magnetism, for example giving rise to memory effects,[1] through to the characterization of metalloenzyme active sites.[2] When the ground state can be described by a total electron spin $S>{}^1\!/_2$, arising from dominant isotropic exchange, the magnetic anisotropy tends to be dominated by the zero-field splitting (ZFS) of the $(2S+1)$-fold multiplet. This is generally assumed to be dominated by the projection of the local ZFSs of the metal ions.[3] When the local spins are $s={}^1\!/_2$ (and have no ZFS) or when they are intrinsically isotropic, such as the ^6S Mn^{II} ion, it is well understood that anisotropic components of the exchange are the main contributions to the ZFS. In contrast, the general significance of the antisymmetric component of the exchange interaction on $S>{}^1\!/_2$ states is not so clear: here we introduce an example where it provides the source of very large ZFS effects.

Antisymmetric exchange (ASE; also known as Dzyaloshinski–Moriya exchange) is the origin of spin canting (weak ferromagnetism) in extended lattices. In terms of molecular systems, ASE was first observed and discussed in trigonal clusters of half-integer spins.[4,5] This is because they provide the simplest discrete systems in which spin frustration can be studied,[6] since antiferromagnetic coupling in an equilateral triangle leads to two degenerate $S={}^1\!/_2$ lowest energy states (^2E term). ASE provides a mechanism for breaking the ^2E degeneracy, and these effects can be quantified by EPR spectroscopy as they are manifested as unusual effective g-values.[3,4] The unusual EPR signatures of some trimetallic Cu[7] and FeS[8] enzymes can be explained by these effects. ASE effects on $S>{}^1\!/_2$ states are much less studied, although it has been proposed as a mechanism for otherwise-forbidden magnetization quantum tunneling steps in Mn_{12} and other single molecule magnets[9] and also for the origin of high-order ZFS effects.[10]

Belinsky[11] and Tsukerblat et al.[12] have calculated the effects of the ASE on the maximum $S={}^3\!/_2$ state (as ground or excited state) in Cu^{II}_3 and V^{IV}_3 triangles. They showed that components of the ASE within the M_3 plane could break the degeneracy, that is, introduce a ZFS. However, in-plane components are symmetry forbidden when the M_3 triangle lies on a mirror plane.[5] They further showed that symmetry-allowed components normal to the triangle do not split the quartet unless there is a large isosceles distortion.[11] Here we show that this can explain the huge ZFSs in the $S>{}^1\!/_2$ ground state of the heterometallic triangle $[Ru_2Mn(O)(tBuCO_2)_6(py)_3]$ ($\{Ru_2Mn\}$, py = pyridine; Figure 1), which we have characterized by multifrequency EPR spectroscopy from 4 to 330 GHz.

$\{Ru_2Mn\}$ and its $\{Fe_2Mn\}$ analogue both crystallize in the $P2_1$ space group with one molecule per asymmetric unit (ESI): the Mn site is not crystallographically resolved. They have the classic structure of basic metal carboxylate triangles,[13] with bridging pivalate and terminal pyridine groups (Figure 1). The acetate analogues of these complexes have been reported,[14,15] and we find similar magnetic susceptibility (χ) behavior. $\{Ru_2Mn\}$ has $\chi T=4.42\,cm^3\,K\,mol^{-1}$ (Figure 2), the

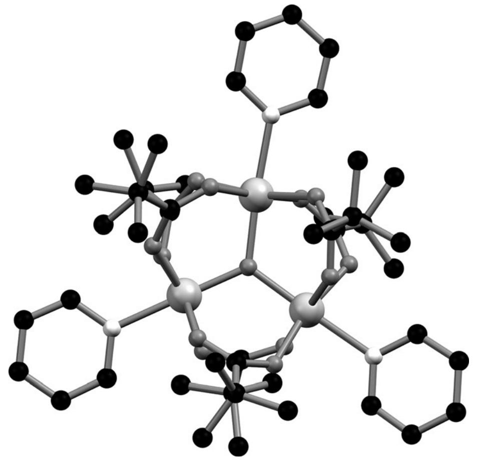

Figure 1. Molecular structure of $\{Ru_2Mn\}$.[26] Scheme: Ru/Mn (large spheres), O (gray), N (white), C (black), H omitted for clarity. Average M···M and M-O distances: 3.36(4) and 1.94(4) Å in $\{Ru_2Mn\}$ and 3.32(4) and 1.91(5) Å in $\{Fe_2Mn\}$, respectively.

---

[*] S. A. Magee, Dr. S. Sproules, Dr. G. A. Timco, N. F. Chilton, Prof. D. Collison, Prof. R. E. P. Winpenny, Prof. E. J. L. McInnes
School of Chemistry and Photon Science Institute
The University of Manchester
Oxford Road, Manchester, M13 9PL (UK)
E-mail: eric.mcinnes@manchester.ac.uk
Dr. A.-L. Barra
Laboratoire National des Champs Magnétiques Intenses
UPR 3228 CNRS, UJF-INSA-UPS, BP 166
38042 Grenoble Cedex 9 (France)

[**] This work was supported by the EPSRC (UK), including the National EPR Facility and Service, and The University of Manchester.

Supporting information for this article is available on the WWW under http://dx.doi.org/10.1002/anie.201400655.

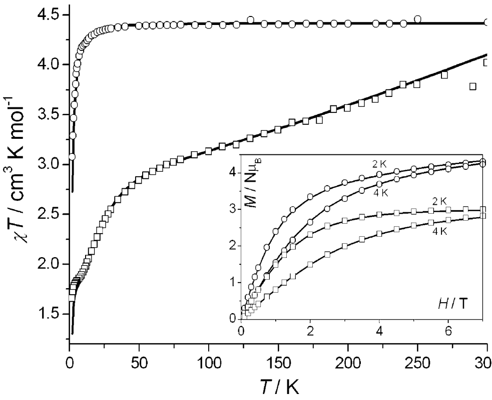

Figure 2. $\chi T(T)$ values for $\{Ru_2Mn\}$ (circles) and $\{Fe_2Mn\}$ (squares) measured in an applied magnetic field (H) of 0.1 T, with simulations (lines) as described in the text. Inset: $M(H)$ at 2 and 4 K.

value expected for an isolated $S = {}^5/_2$ state, hence the magnetic properties appear at first sight to be those of the isolated Mn^{II} ion. Using the isotropic Hamiltonian $\hat{H}_{iso}$ [Eq. (1)]:

$$\hat{H}_{iso} = \sum\nolimits_i g_i\beta\hat{\mathbf{s}}_i H - 2J_1\left(\hat{\mathbf{s}}_1\cdot\hat{\mathbf{s}}_2\right) - 2J_2\left(\hat{\mathbf{s}}_1\cdot\hat{\mathbf{s}}_3+\hat{\mathbf{s}}_2\cdot\hat{\mathbf{s}}_3\right) \tag{1}$$

where $s_1 = s_2 = {}^1/_2$ (Ru^{III}, low-spin d^5) and $s_3 = {}^5/_2$ (Mn^{II}, high-spin d^5), this corresponds to the $|0,s_3\rangle$ ground state ($|S_{12},S\rangle$). A simple Kambé treatment gives this ground state for $J_1/J_2 > 3.5$, with the first excited state ($|1,3/2\rangle$) at a relative energy of $7J_2 - 2J_1$. Test calculations show that $|J_1|$ must be greater than ca. 10^3 cm^{-1} and that J_1/J_2 must be greater than ca. 10 for there to be no evidence of excited-state population in $\chi T(T)$ at high temperature. Large $|J_1|$ values are justified by the large radial extent of the 4d wavefunctions, and indeed direct overlap as opposed to super-exchange is possible. Couplings of this magnitude have been observed in homometallic Ru^{III} cages.[16]

Fitting the low-temperature drop in $\chi T(T)$, and magnetization (M) data (Figure 2), for an isolated $S = {}^5/_2$ with $\hat{H}_{ZFS}$ [Eq. (2)], gives the axial ZFS parameter $|D| = 3.0$ cm^{-1} ($E = 0$, with fixed $g = 1.98$).[17]

$$\hat{H}_{ZFS} = g_i\beta\hat{\mathbf{S}}H + D\left(\hat{S}_z^2 - \frac{S(S+1)}{3}\right) + E\left(\hat{S}_x^2 - \hat{S}_y^2\right) \tag{2}$$

This is much larger than estimated previously for the acetate analogue by low-frequency EPR spectroscopy;[15] therefore, we have measured the value of D directly by high-frequency EPR spectroscopy.[18] Spectra at low frequencies are those of an axial effective spin ${}^1/_2$ with $g_{\mathrm{eff},\perp} \approx 6$ and $g_{\mathrm{eff},\parallel} \approx 2$, consistent with a ground-state $M = \pm{}^1/_2$ Kramers doublet, with resolved ^{55}Mn hyperfine for frozen solution samples (Figure 3a and see Figure S1 in the Supporting Information). Spectra recorded at 220 and 330 GHz (Figure 3) unambiguously define the $S = {}^5/_2$ multiplet, and simulation[19] with $\hat{H}_{ZFS}$ gives $D = +2.9$ cm^{-1} ($E = 0$) with $g = 1.98$ (see Figure S2 in the Supporting Information).

In this simple model the ZFS of the $|0,5/2\rangle$ state should correspond to that of the isolated Mn^{II} site. However, this is absurd: the largest values reported for six-coordinate Mn^{II}

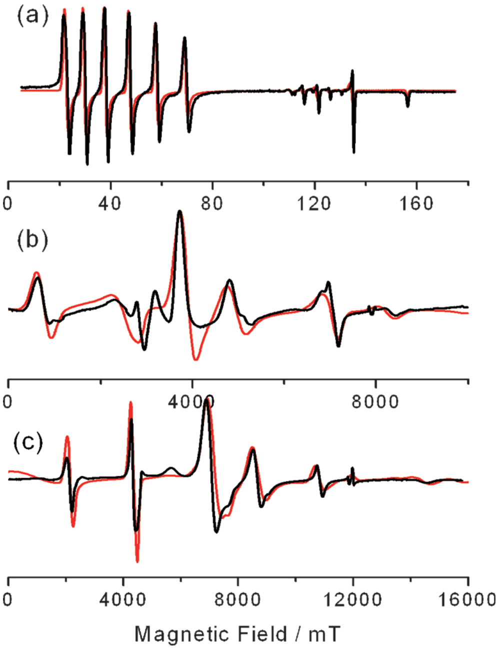

Figure 3. EPR spectra of $\{Ru_2Mn\}$ at 10 K, measured at: a) 3.87 GHz on a CH_2Cl_2/toluene solution; b) 220.8; and c) 331.2 GHz on a polycrystalline sample. Simulations (red) based on Hamiltonian $\hat{H}_{iso} + \hat{H}_{anti}$ with the parameters in the text; the S-band simulation included an isotropic ^{55}Mn hyperfine coupling ($A\hat{\mathbf{s}}_3\cdot\hat{\mathbf{I}}_3$; $I_3 = {}^5/_2$) of $|A| = 85\times10^{-4}$ cm^{-1} (typical for this coördination environment[20]). Gaussian linewidth parameters: a) 15 (x,y) and 3 (z) G, with an A-strain of 2%; b,c) 1500 G Gaussian linewdith with 5% strain in d_2^z (see text for definition of the z direction).

ions with O,N donor sets are $|D| < 0.2$ cm^{-1}.[20] To test the model we have prepared and studied the equivalent 3d complex $\{Fe_2Mn\}$ in which the Mn^{II} ion has the same coordination environment. Fitting $\chi T(T)$ for $\{Fe_2Mn\}$ to $\hat{H}_{iso}$ with $s_1 = s_2 = {}^5/_2$ gives $J_1 = -63.5$ and $J_2 = -21.9$ cm^{-1} with $g = 2.0$ (Figure 2), similar to its acetate analogue.[21] This gives the $|1,3/2\rangle$ ground state, as confirmed by low-temperature magnetization and EPR measurements. Modeling the latter with $\hat{H}_{ZFS}$ for $S = {}^3/_2$ gives $D = +0.25$, $|E| = 0.04$ cm^{-1} (fixed $g = 2.0$; Figures 2 and 4). While the $|1,3/2\rangle$ ZFS has contributions from all three metal ions, assuming it arises entirely from Mn^{II} (an over-estimation) gives $D_{Mn} = +0.13$ cm^{-1}. This is in the range known for O,N-donor six-coordinate Mn^{II},[20] but negligible compared to the ground-state ZFS of $\{Ru_2Mn\}$. Hence $\{Ru_2Mn\}$ has a contribution of about 3 cm^{-1} to its ZFS from another source.

Given the predictions for ASE effects in the high-spin state of $s = {}^1/_2$ triangles,[11] we have investigated this model by the Hamiltonian $\hat{H}_{iso} + \hat{H}_{anti}$, where $\mathbf{d}_i$ are the ASE vectors,[4] and $\hat{H}_{anti}$ is defined in Equation (3).

$$\hat{H}_{anti} = \mathbf{d}_1\left(\hat{\mathbf{s}}_1\times\hat{\mathbf{s}}_2\right) + \mathbf{d}_2\left(\hat{\mathbf{s}}_2\times\hat{\mathbf{s}}_3+\hat{\mathbf{s}}_3\times\hat{\mathbf{s}}_1\right) \tag{3}$$

If we neglect the torsion angles of the terminal pyridine ligands, then $\{Ru_2Mn\}$ is an isosceles triangle with C_{2v} symmetry. We define the normal to the trimetallic plane as the z axis to maintain consistency with the literature reports

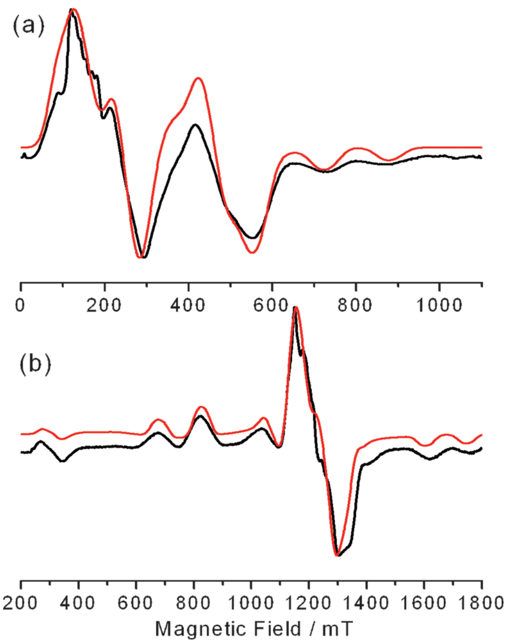

Figure 4. EPR spectra of polycrystalline {Fe_2Mn} measured at 10 K and a) 9.76 and b) 33.97 GHz (5 K), with simulations (red) based on Hamiltonian $\hat{H}_{ZFS}$ with the parameters in the text. Gaussian linewidth of 300 G.

on M_3 triangles. In this case, all three metal–metal vectors lie on a mirror plane and the only non-zero components of $\mathbf{d}_i$ are d_i^z. Such components do not lead to ZFS in the high-spin states of equilateral triangles.[11,12] In our case we have a system that is isosceles not only in terms of the strength of the J coupling (often seen in homometallic triangles), but in the identity of the spins themselves.

Hamiltonian $\hat{H}_{iso}$ gives the 24 × 24 energy matrix comprising the ground $|0,5/2\rangle$ (with eigenvalue $+3J_1/2$) and excited $|1,3/2\rangle$ $(-J_1/2+7J_2)$, $|1,5/2\rangle$ $(-J_1/2+2J_2)$, and $|1,7/2\rangle$ $(-J_1/2-5J_2)$ states. Applying $\hat{H}_{anti}$, with only $d_i^z \neq 0$, as a perturbation to this coupled basis gives the non-zero matrix elements (labeling states as $|S_{12},S,M\rangle$):

$$\left\langle 1,\tfrac{7}{2},\pm\tfrac{5}{2}\right|\hat{H}_{anti}\left|0,\tfrac{5}{2},\pm\tfrac{5}{2}\right\rangle = -i\,\frac{d_1^z-5d_2^z}{\sqrt{14}}$$

$$\left\langle 1,\tfrac{5}{2},\pm\tfrac{5}{2}\right|\hat{H}_{anti}\left|0,\tfrac{5}{2},\pm\tfrac{5}{2}\right\rangle = \pm i\sqrt{5}\,\frac{d_1^z+2d_2^z}{2\sqrt{7}}$$

$$\left\langle 1,\tfrac{7}{2},\pm\tfrac{3}{2}\right|\hat{H}_{anti}\left|0,\tfrac{5}{2},\pm\tfrac{3}{2}\right\rangle = -i\sqrt{10}\,\frac{d_1^z-5d_2^z}{2\sqrt{21}}$$

$$\left\langle 1,\tfrac{5}{2},\pm\tfrac{3}{2}\right|\hat{H}_{anti}\left|0,\tfrac{5}{2},\pm\tfrac{3}{2}\right\rangle = \pm 3i\,\frac{d_1^z+2d_2^z}{2\sqrt{35}}$$

$$\left\langle 1,\tfrac{3}{2},\pm\tfrac{3}{2}\right|\hat{H}_{anti}\left|0,\tfrac{5}{2},\pm\tfrac{3}{2}\right\rangle = i\,\frac{d_1^z+7d_2^z}{\sqrt{15}}$$

$$\left\langle 1,\tfrac{7}{2},\pm\tfrac{1}{2}\right|\hat{H}_{anti}\left|0,\tfrac{5}{2},\pm\tfrac{1}{2}\right\rangle = -i\,\frac{d_1^z-5d_2^z}{\sqrt{7}}$$

$$\left\langle 1,\tfrac{5}{2},\pm\tfrac{1}{2}\right|\hat{H}_{anti}\left|0,\tfrac{5}{2},\pm\tfrac{1}{2}\right\rangle = \pm i\,\frac{d_1^z+2d_2^z}{2\sqrt{35}}$$

$$\left\langle 1,\tfrac{3}{2},\pm\tfrac{1}{2}\right|\hat{H}_{anti}\left|0,\tfrac{5}{2},\pm\tfrac{1}{2}\right\rangle = i\,\frac{d_1^z+7d_2^z}{\sqrt{10}}$$

There are no first-order corrections to the eigenvalues, but each ground-state M component mixes with all excited states with $\Delta M = 0$. The three Kramers doublets are separated and, to second order, the $|M| = {}^1\!/_2$ to ${}^3\!/_2$ gap is half the ${}^3\!/_2$ to ${}^5\!/_2$ gap. This is the form of an isolated $S = {}^5\!/_2$ state under Hamiltonian (2), with separations of $2D$ and $4D$, respectively. To second order, D is then given by Equation (4),

$$D = \frac{-\left(2d_2^zJ_1+d_1^zJ_2\right)^2}{(2J_1-7J_2)(2J_1-2J_2)(2J_1+5J_2)} \tag{4}$$

where the denominator is the product of the gaps to the three excited states.

Excellent simulations of the EPR spectra (Figure 3 and see Figure S3 in the Supporting Information), including variable-temperature and hyperfine effects, are obtained by full diagonalization of $\hat{H}_{iso}+\hat{H}_{anti}$ (with $g_{\mathrm{Mn}} = 1.98$ and $g_{\mathrm{Ru}} = 2.0$; the simulations are insensitive to the latter), and fits to the low-temperature $\chi T(T)$ and $M(H)$ are indistinguishable from those in Figure 2. For these calculations we have taken $J_1 = -1000\ \mathrm{cm}^{-1}$ with $J_1/J_2 = 10$ (see above). Clearly, more than one set of d_1^z,d_2^z components can generate a given D value. If we take $d_1^z = 0$, then we find $d_2^z = 66\ \mathrm{cm}^{-1}$ (Figure 3; calculations are insensitive to the sign of d_i^z); much larger values of d_1^z are required to generate equivalent D values [see Eq. (4)]. Adjustment of J_1 and J_2 will give different d_i^z values, but the conclusion does not change: very large ZFS effects (several cm^{-1}) have been introduced to the $S > {}^1\!/_2$ ground state by ASE effects in second-order. (There are also higher-order contributions: the calculated $|M| = {}^5\!/_2$ to ${}^3\!/_2$ gap is not exactly double the ${}^3\!/_2$ to ${}^1\!/_2$ gap from diagonalization using $\hat{H}_{iso}+\hat{H}_{anti}$.) Moreover, the simple description of the magnetic properties of {Ru_2M} as being "those of the isolated M ion" is wrong.

The ASE parameters we have found here are entirely reasonable: d_i^z values of greater than $100\ \mathrm{cm}^{-1}$ have been found for antiferromagnetically coupled Cu^{II} triangles.[5,7,22] It has been argued that the latter are due to the favorable alignment of ground- and excited-state d orbitals,[7] because ASE arises from exchange between the electronic ground state of one ion and the excited state of another through spin–orbit coupling (SOC). In {Ru_2M}, the ASE will be favored both by the large SOC of Ru^{III}, and the strong exchange interactions arising from the large radial extent of the 4d orbitals. The perturbative expressions above show that this can also be viewed as mixing of the ground-state Mn^{II} functions ($S_{12} = 0$) with the "ferromagnetic" excited state ($S_{12} = 1$) of the {Ru_2} unit. This is equivalent to an alternative description of the electronic structure proposed for some oxo-bridged Ru^{III} oligomers, where direct exchange between the 4d functions results in delocalized singlet and "low lying" (in electronic spectroscopy terms) triplet states.[23,24]

In summary, we have shown the ASE interaction can lead to very large spin ground-state ZFSs in polymetallic complexes, even through a second-order perturbation on the isotropic exchange. The model reproduces spectroscopic observations across two orders of magnitude in field/frequency regime of EPR spectroscopy. The results show that these effects cannot be ignored, particularly when 2nd and 3rd row metal ions are involved, as is becoming popular as a route to introduce magnetic anisotropy into molecular magnets. Furthermore, it is possible that ASE is much more widespread than generally imagined in coupled systems, and assigned to anisotropic exchange or local ZFS effects; for example, a ground state $D = 0.25\ \mathrm{cm}^{-1}$ for $\{Fe_2Mn\}$ can equally well be derived from $d_2^z = 0.67\ \mathrm{cm}^{-1}$, similar to values observed in $\{Fe_3\}$ triangles.[5] This is important because different anisotropy terms in the spin Hamiltonian result in different mixing between ground and excited states, which have important consequences for phenomena such as magnetic relaxation, including, as discussed by others, a possible origin of "forbidden" quantum tunneling steps and avoided crossings observed in several molecular nanomagnets.[9,25]

Received: January 21, 2014

Keywords: antisymmetric exchange · electronic structure · EPR spectroscopy · exchange coupling · zero-field splitting

[1] R. Sessoli, D. Gatteschi, J. Villain, *Molecular Nanomagnets*, Oxford University Press, Oxford, **2006**.
[2] W. R. Hagen, *Biomolecular EPR Spectroscopy*, CRC Press, Taylor and Francis Group, **2009**.
[3] A. Bencini, D. Gatteschi, *EPR of Exchange Coupled Systems*, Springer, Berlin, **1990**.
[4] B. S. Tsukerblatt, M. I. Belinskii, A. V. Ablov, *Dokl. Akad. Nauk SSSR* **1971**, *201*, 1410; M. I. Belinskii, B. S. Tsukerblatt, A. V. Ablov, *Mol. Phys.* **1974**, *28*, 283; B. S. Tsukerblat, B. Y. Kuyavskaya, M. I. Belinskii, A. V. Ablov, V. M. Novotortsev, V. T. Kalinnkov, *Theor. Chim. Acta* **1975**, *38*, 131; Y. V. Rakitin, Y. V. Yablokov, V. V. Zelentsov, *J. Magn. Reson.* **1981**, *43*, 288.
[5] For a recent review, see R. Boča, R. Herchel, *Coord. Chem. Rev.* **2010**, *254*, 2973.
[6] O. Kahn, *Chem. Phys. Lett.* **1997**, *265*, 109.
[7] J. Yoon, E. I. Solomon, *Inorg. Chem.* **2005**, *44*, 8076; J. Yoon, E. I. Solomon, *Coord. Chem. Rev.* **2007**, *251*, 379.
[8] Y. Sanakis, A. L. Macedo, I. Moura, J. J. G. Moura, V. Papaefthymiou, E. Münck, *J. Am. Chem. Soc.* **2000**, *122*, 11855; F. Tiago de Oliveira, E. L. Bominaar, J. Hirst, J. A. Fee, E. Münck, *J. Am. Chem. Soc.* **2004**, *126*, 5338.
[9] M. I. Katsnelson, V. V. Dobrovitski, B. N. Harmon, *Phys. Rev. B* **1999**, *59*, 6919; I. Chiorescu, R. Giraud, A. G. M. Jansen, A. Caneschi, B. Barbarba, *Phys. Rev. Lett.* **2000**, *85*, 4807; C. M. Ramsey, E. del Barco, S. Hill, S. J. Shah, C. C. Beedle, D. N. Hendrickson, *Nat. Phys.* **2008**, *4*, 277; S. Bahr, C. J. Milios, L. F. Jones, E. K. Brechin, V. Mosser, W. Wernsdorfer, *Phys. Rev. B* **2008**, *78*, 132401.
[10] N. Kirchner, J. van Slageren, B. Tsukerblat, O. Waldmann, M. Dressel, *Phys. Rev. B* **2008**, *78*, 094426.
[11] M. I. Belinksy, *Inorg. Chem.* **2008**, *47*, 3521; M. I. Belinksy, *Inorg. Chem.* **2008**, *47*, 3532.
[12] B. Tsukerblat, A. Tarantul, A. Müller, *Phys. Lett. A* **2006**, *353*, 48.
[13] R. D. Cannon, R. P. White, *Prog. Inorg. Chem.* **1988**, *36*, 195.
[14] A. Ohto, Y. Sasaki, T. Ito, *Inorg. Chem.* **1994**, *33*, 1245; H. Kobayashi, N. Uryû, R. Miyamoto, Y. Ohba, M. Iwaizumi, Y. Sasaki, A. Ohto, T. Ito, *Bull. Chem. Soc. Jpn.* **1995**, *68*, 2551.
[15] H. Kobayashi, N. Uryû, I. Mogi, R. Miyamoto, Y. Ohba, M. Iwaizumi, Y. Sasaki, A. Ohto, M. Suwabe, T. Ito, *Bull. Chem. Soc. Jpn.* **1996**, *69*, 3163.
[16] A. Upadhyay, J. Rajprohit, M. K. Singh, R. Dubey, A. K. Srivastava, A. Kumar, G. Rajaraman, M. Shanmugam, *Chem. Eur. J.* **2014**, DOI: 10.1002/chem.201304826.
[17] Modeling of magnetic data used PHI software, see N. F. Chilton, R. P. Anderson, L. D. Turner, A. Soncini, K. S. Murray, *J. Comput. Chem.* **2013**, *34*, 1164.
[18] On a home-built instrument: A. L. Barra, A. K. Hassan, A. Janoschka, C. L. Schmidt, V. Schünemann, *Appl. Magn. Reson.* **2006**, *30*, 385.
[19] EPR analysis and simulations used Weihe's SimEPR, with some calculations using routines as described by Piligkos et al., see C. J. H. Jacobsen, E. Pederson, J. Villadsen, H. Weihe, *Inorg. Chem.* **1993**, *32*, 1216; S. Piligkos, E. Bill, D. Collison, E. J. L. McInnes, G. A. Timco, H. Weihe, R. E. P. Winpenny, F. Neese, *J. Am. Chem. Soc.* **2007**, *129*, 760; S. Piligkos, H. Weihe, E. Bill, F. Neese, H. El Mkami, G. M. Smith, D. Collison, G. Rajaraman, G. A. Timco, R. E. P. Winpenny, E. J. L. McInnes, *Chem. Eur. J.* **2009**, *15*, 3152.
[20] C. Duboc, M.-N. Collomb, F. Neese, *Appl. Magn. Reson.* **2010**, *37*, 229.
[21] A. B. Blake, A. Yavari, W. E. Hatfield, C. N. Sethulekshmi, *J. Chem. Soc. Dalton Trans.* **1985**, 2509.
[22] For recent examples, see A. Escuer, G. Vlahopoulou, F. Lloret, F. A. Mautner, *Eur. J. Inorg. Chem.* **2014**, 83.
[23] T. R. Weaver, T. J. Meyer, S. A. Adeyemi, G. M. Brown, R. P. Eckberg, W. E. Hatfield, E. C. Johnson, R. W. Murray, D. Untereker, *J. Am. Chem. Soc.* **1975**, *97*, 3039.
[24] J. A. Baumann, D. J. Salmon, S. T. Wilson, T. J. Meyer, W. E. Hatfield, *Inorg. Chem.* **1978**, *17*, 3342; Y. Sasaki, A. Tokiwa, T. Ito, *J. Am. Chem. Soc.* **1987**, *109*, 6341.
[25] F. Cinti, M. Affronte, A. G. M. Jansen, *Eur. Phys. J. B* **2002**, *30*, 461.
[26] CCDC 926362 and 926363 contain the supplementary crystallographic data for this paper. These data can be obtained free of charge from The Cambridge Crystallographic Data Centre via www.ccdc.cam.ac.uk/data_request/cif.